



Large Tunable 16-Tupled Millimeter Wave Generation Utilizing Optical Carrier Suppression With a Tunable Sideband Suppression Ratio

Asha* and Sandeep Dahiya

Department of ECE, Faculty of Engineering and Technology, BPS Women University, Khanpur Kalan, Sonapat, India

Coping up with the rising bandwidth demands for 5G ultra-high speed applications, utilizing millimeter (MM) wave spectrum for data transmission over the radio over a fiber-based system is the ideal approach. In this study, a highly conversant and spectrally pure photonic generation of a 16-tupled MM wave signal using a series-connected DD-MZM with a lower modulation index, a splitting ratio, and a wider tunable range is presented. A 160-GHz MM wave is generated through a double sideband optical carrier suppression technique having an optical sideband suppression ratio (OSSR) of 69 dB and a radio frequency sideband suppression ratio (RSSR) of 40 dB. However, the OSSR and the RSSR are tunable with values greater than 15 dB when the modulation index (M.I.) varies from 2.778 to 2.873, $\pm 8^\circ$ phase drift, and a 15-dB enhancement in the OSSR with a wider nonideal parameter variation range giving acceptable performance can be seen in the model as compared with previous research works.

OPEN ACCESS

Edited by:

Santosh Kumar,
Liaocheng University, China

Reviewed by:

Sharda Vashisth,
The NorthCap University, India
Dhramendra Yadav,
Bikaner Technical University, India

*Correspondence:

Asha
ashabalhara89@gmail.com

Specialty section:

This article was submitted to
Optics and Photonics,
a section of the journal
Frontiers in Physics

Received: 25 July 2021

Accepted: 17 August 2021

Published: 18 October 2021

Citation:

Asha and Dahiya S (2021) Large
Tunable 16-Tupled Millimeter Wave
Generation Utilizing Optical Carrier
Suppression With a Tunable Sideband
Suppression Ratio.
Front. Phys. 9:747030.
doi: 10.3389/fphy.2021.747030

Keywords: millimeter wave generation, radio over fiber system, 16 tupling, OSSR, RSSR, filterless, optical carrier suppression

INTRODUCTION

For supporting multi gigabit per second (gbps) wireless connectivity and resolving spectrum shortage, 5G uses higher frequencies from an MM wave range (30–300 GHz) for signal transmission. However, the generation and transmission of MM wave signals is a troublesome process as these high-frequency signals apart from providing a wide bandwidth limits the transmission distance due to propagation losses. So, in order to cope up with this issue, the MM wave signal is first generated by modulating a low-frequency electrical signal over an optical carrier coming from a light source at a central station (CS) and then transmitting it to the base station (BS). This technique is named as millimeter wave-based radio over the fiber (i.e., MMoF) system. This fiber-based system provides low insertion and transmission losses with being immune toward electromagnetic interference.

The basic requirement for designing an efficient MMoF system is to modulate the RF signal for generating a desired MM wave signal with suppressing all other unwanted signals. The MM waves can be generated in two domains: 1) electrical and 2) optical or photonic. However, MM wave signal generation in a photonic domain is best suited in comparison to their electrical counterparts due to lower phase noise, lower equipment requirement, higher spectral purity, a wider tunable range, and a larger transmission distance [1]. Several different techniques have been discussed in the past for photonic MM wave signal generation which include a direct

TABLE 1 | Literature review of frequency 16-tupled MM wave generation based on different parameters.

Author (Year)	Working Principle	Parameters							
		OSSR (dB)	RSSR (dB)	Filters	Modulation index	Cost effective	Power efficient	Tunability	O/P freq Generated (GHz)
Zihang Zhu [6] (2015)	Two-cascaded dual parallel MZM	21.5	38	No	2.265	No	No	Low	60
K. Esakki Muthu [10] (2016)	Parallel combination of two-cascaded MZM	20	28	Yes	3.14	Yes	Yes	Low	60
M. Baskaran [14] (2018)	Cascaded MZM	54	42	No	2.827	Yes	No	High	80
Dongfei Wang [13] (2019)	Two-cascaded MZM	31.35	24.11	Yes	7.59 (very high)	Yes	Yes	Low	160
Aasif Bashir Dar [9] (2020)	Cascaded parallel MZM	64	31	No	2.79–2.86	No	No	Low	80
Proposed Scheme (2021)	Series MZM configuration	69	40	No	2.778–2.873	Yes	Yes	High	160

modulation [1], an external modulation [2], optical heterodyning [3], Stimulated Brillouin scattering (SBS) [4] etc.

Among the above-stated techniques, the generation method utilizing an external modulation through a Mach-Zehnder Modulator (MZM) is the most reliable one as it offers optical harmonics generation with a higher frequency multiplication factor (FMF), stability, and greater tunability as mentioned in our previous review study in [5]. When an RF signal drives an external modulator, several optical harmonics are generated due to its nonlinear transfer function. By the beating of these harmonics at photodetector, MM wave signals are generated. The main technical challenge in the frequency multiplication (FM) approach is generating required optical harmonics while eliminating unwanted optical harmonics with higher conversion efficiency. So far, FMF of 2, 4, 6, 8, 10, 12, 14, and 16 have been proposed. However, MM wave generation utilizing a high FMF is quite efficient as it eliminates the requirement of high-frequency operated local oscillator (LO) operating at CS.

Recently, several generation techniques have been reported with a 16 FMF utilizing a two-cascaded dual parallel MZM configuration [6–8], parallel combination of two cascaded MZM [9], cascaded parallel MZM [10, 11], and a feedforward modulation [12]. Dongfei Wang [13] proposed a generation method with a two-cascaded MZM but with a higher modulation index ($>>7$) requiring a high voltage radio frequency signal which in turn increases the system sensitivity. These schemes employ a filter for generating desired harmonics which not only increases system complexity but also reduces its tunability range and conversion efficiency. A filterless method has been proposed by the authors of reference [14] using cascaded MZM with an infinite extinction ratio which is not practically realizable. These techniques lead to partial cancellation of undesired harmonics and thus provide a lower sideband suppression ratio (SBSR) at the transmitting side leading to detect unwanted MM waves which deteriorate the system performance and also lower the spectral purity that is not desired for MM wave applications. The detailed review of these configurations is provided in **Table 1**.

In the present study, a cost-effective and spectrally pure 16-tupled MM wave frequency is generated by completely suppressing all the other undesired harmonics except eighth-order sideband (SB) using a series connection of a quad dual drive MZM (DD-MZM) and electrical phase shifters for optimizing biases of MZM and enhancing the OSSR and the RSSR by utilizing a lower modulation index and

the extinction and the splitting ratio. A Theoretical analysis along with designing a simulation model is also carried out for understanding the cancellations of all other harmonics. The OSSR of 69 dB and the RSSR of 40 dB are obtained. The effectiveness of the 16-tupled generated MM wave is assessed by analyzing the effect of the MZM extinction ratio, the splitting ratio, the modulation index, and modulating frequency of the RF signal on the OSSR and the RSSR. The rest of the paper is structured as follows. The design principle of the proposed frequency 16 tupled structure is described in **Section 2**. The simulation results with the impact of non-ideal parameter variation on the SBSR are discussed in **Section 3** and finally the conclusion is presented in **Section 4**.

DESIGN PRINCIPLE

The MWPL is built using the OptiSystem version 17.0.0. **Figure 1** shows a schematic diagram of the proposed filterless MM wave generation with frequency 16 tupling. For generating MM wave with FMF of 16, \pm eighth-order SBs must hit the photodetector (PD). In order to obtain this, MZM should be biased at MXTP which provides a carrier and only even order SBs after modulation. Furthermore, obtaining pure \pm eighth-order SBs is quite challenging because several other unwanted spurious SBs are also generated.

For suppressing all other spurious harmonics, subsequent measures are adopted in the proposed scheme as: 1) setting MZM at MXTP for suppressing all the odd order SBs and generating only even order SBs, 2) controlling the M.I. of the MZM to let the power of sidebands greater than ± 10 th order sidebands return to zero or is negligible, and 3) adjusting the electrical phase shift of the RF driving signal between the MZM and insertion loss of modulator so as to suppress the carrier and eliminate all the other $(2n-2)^{\text{th}}$ order sidebands except \pm eighth-order SBs. The detailed principle of the proposed scheme is mentioned below.

It utilizes a laser diode (LD), an RF signal generator, electrical phase shifters, a photodiode, optical amplifiers, and a DD-MZM. A continuous wave laser (CWL) with frequency ω_c emits the light signal which acts as a carrier signal defined as follows:

$$V_{in} = V_c (\cos \omega_c t). \quad (1)$$

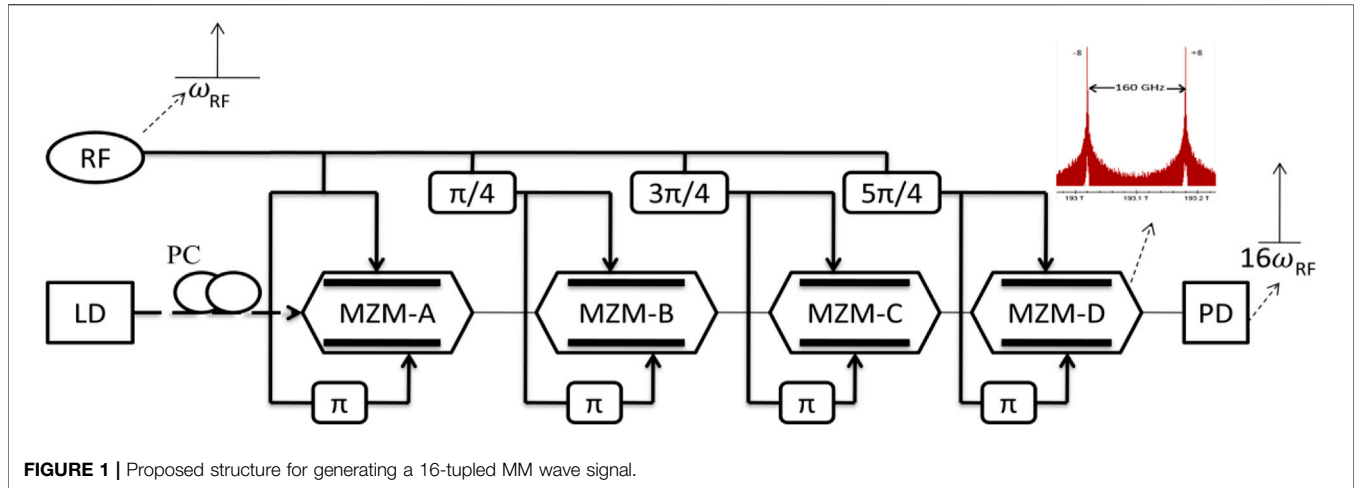


FIGURE 1 | Proposed structure for generating a 16-tupled MM wave signal.

Here, V_c is the amplitude of the carrier signal.

This light carrier wave after being polarization controlled (PC) is transmitted to the first intensity modulator, that is, MZM-A triggered by RF LO which produces a single RF tone of frequency, ω_{rf} , given by the following:

$$V_1 = V_{rf} (\cos \omega_{rf} t), \tag{2}$$

where V_{rf} is the amplitude of the input RF signal.

Odd order Harmonics Elimination

The transfer function of a DD-MZM is expressed as follows:

$$E_{MZM-A}(t) = \frac{\beta}{2} E_c e^{j\omega_c t} \{ \chi e^{-jm_a \sin \omega_{RF} t} + (1 - \chi) e^{jm_a \sin \omega_{RF} t} \}, \tag{3}$$

where $m_a = \frac{\pi V_{RF}}{V_\pi}$ is the M.I.,

V_{RF} is the switching RF voltage, V_π is the half wave voltage of MZM, and β is the insertion loss of MZM.

$x = \frac{(1 - \frac{1}{\sqrt{\beta}})}{2} \{ \mu_r = 10^{(MZM \text{ extinction ratio})/10} \}$ is the splitting ratio of upper and lower arms of MZM.

However, using the Jacobi–Anger expansion,

$$\begin{aligned} e^{jmsin\Phi} &= \sum_{k=-\infty}^{k=\infty} J_k(m) e^{jk\Phi} \text{ and } e^{jmc\cos\Phi} \\ &= \sum_{k=-\infty}^{k=\infty} (-1)^k J_k(m) e^{jk\Phi}. \end{aligned} \tag{4}$$

The transfer function can be rewritten as follows:

$$E_{MZM}(t) = \beta E_c \left[\sum_{k=-\infty}^{k=\infty} (-1)^k J_k(m) e^{j(\omega_c + k\omega_{RF})t} \right], \tag{5}$$

$$\begin{aligned} E_{MZM}(t) &= \beta E_c \left[J_0(m_a) e^{j\omega_c t} - J_1(m_a) \{ e^{j(\omega_c - \omega_{RF})t} + e^{j(\omega_c + \omega_{RF})t} \} \right. \\ &\quad + J_2(m_a) \{ e^{j(\omega_c - 2\omega_{RF})t} + e^{j(\omega_c + 2\omega_{RF})t} \} \\ &\quad \left. - J_3(m_a) \{ e^{j(\omega_c - 3\omega_{RF})t} + e^{j(\omega_c + 3\omega_{RF})t} \} + \dots \dots \dots \right]. \end{aligned} \tag{6}$$

As the Li-NbO₃ DD-MZM has a nonlinear characteristic response, the modulated output optical signal consists of a carrier along with multiple sidebands symmetrically located around it as depicted in Eq. 6. The amplitude and number of sidebands generated around the carrier can be controlled by varying m_a which in turn depends on V_{RF} and V_π . In order to suppress the odd order SBs, the first modulator is biased at MXTP by applying the bias voltages to the upper and lower arms of the modulator such that $V_{bias} = V_{bias1} - V_{bias2} = 0$ with a π phase difference between the RF signals fed to the arms of the modulator.

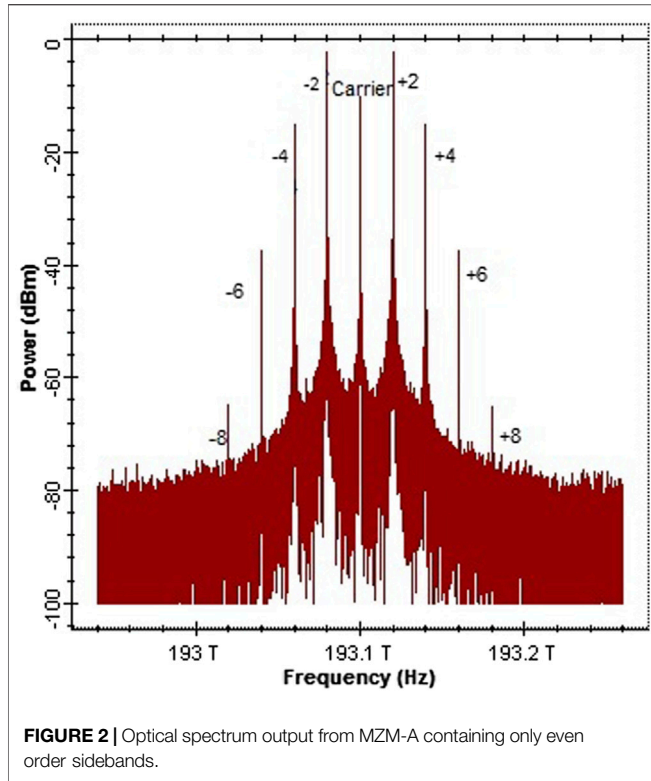
$$\begin{aligned} E_{MZM-A}(t) &= \beta E_c e^{j\omega_c t} \left[J_0(m_a) + J_2(m_a) \{ e^{j2\omega_{RF}t} + e^{-j2\omega_{RF}t} \} \right. \\ &\quad + J_4(m_a) \{ e^{j4\omega_{RF}t} + e^{-j4\omega_{RF}t} \} + J_6(m_a) \{ e^{j6\omega_{RF}t} \\ &\quad \left. + e^{-j6\omega_{RF}t} \} + J_8(m_a) \{ e^{j8\omega_{RF}t} + e^{-j8\omega_{RF}t} \} \right]. \end{aligned} \tag{7}$$

The above equation clearly depicts that there are $2n^{th}$ order, that is, even SBs generated from the first modulator, and the corresponding optical spectrum is shown in Figure 2.

Suppressing (2n-2)th Order Sidebands

For suppressing $(2n-2)^{th}$ order sidebands, except the desired \pm eighth sidebands, an MZM-A output is fed to the second one, which in turn goes to the third and then to the fourth in such a manner that all the modulators are driven with the RF signal with a suitable phase shift between the two consecutive modulators such that the output from the last modulator only contains the desired \pm eighth-order SB and the separation between the desired sidebands is the 16th multiple of input RF.

The modulated output from MZM-A is sent to MZM-B which is triggered by an RF signal with a 45° phase difference such that $V_2 = V_{rf} (\cos \omega_{rf} t + \pi/4)$ is mathematically expressed in Eq. 6 as follows:



$$E_{MZM-B}(t) = \frac{\beta^2}{2} E_c e^{jn/4} \left[\sum_{k=-\infty}^{k=\infty} J_k^2(m_a) e^{j(\omega_c + 2k\omega_{RF})t + k\pi} \right]. \quad (8)$$

This output from MZM-B is an input to the third MZM triggered by the RF signal with an electrical phase difference of 135°.

$$E_{MZM-C}(t) = \beta E_{MZM-B}(t) \{ J_0(m_a) - J_2(m_a) \} \{ e^{j2\omega_{RF}t} + e^{-j2\omega_{RF}t} \} + J_4(m_a) \{ e^{j4\omega_{RF}t} + e^{-j4\omega_{RF}t} \} - J_6(m_a) \{ e^{j6\omega_{RF}t} + e^{-j6\omega_{RF}t} \} + J_8(m_a) \{ e^{j8\omega_{RF}t} + e^{-j8\omega_{RF}t} \} - J_{10}(m_a) \{ e^{j10\omega_{RF}t} + e^{-j10\omega_{RF}t} \} + J_{12}(m_a) \{ e^{j12\omega_{RF}t} + e^{-j12\omega_{RF}t} \}. \quad (9)$$

This output is fed to the last modulator, that is, MZM-D which is driven by the RF signal phase shifted by 225°. By providing this phase shift, $J_2(m_a)$, $J_4(m_a)$, and $J_6(m_a)$ terms turn into zero and other higher order harmonics, such as $J_{10}(m_a)$ and $J_{12}(m_a)$, have extremely low power which can be neglected.

Tunable Optical Carrier Suppression

By properly adjusting the modulation index, the carrier could be suppressed completely which results into power saving and efficient transmission leaving behind the optical spectrum with only the eighth-order SB as depicted in **Figure 3**. The MZM-D output can be stated mathematically as follows:

$$E_{MZM-D}(t) = \frac{\beta^4}{2} J_8^2(m_a) E_c e^{j\omega_c t} \{ e^{j8\omega_{RF}t} + e^{-j8\omega_{RF}t} \}. \quad (10)$$

This output is then detected at the receiver side through the PIN photodiode whose photocurrent is given by the following equation:

$$I_{ph}(t) = \mu_{ph} |E_{MZM-D}(t)| * |E_{MZM-D}(t)|^*, \quad (11)$$

$$I_{ph}(t) = \mu_{ph} \left\{ \frac{\beta}{2} E_c [J_{-8}(m_a) e^{j(\omega_c - 8\omega_{RF})t} + J_8(m_a) e^{j(\omega_c + 8\omega_{RF})t}] \right\} * \left\{ \frac{\beta}{2} E_c [J_{-8}(m_a) e^{j(\omega_c - 8\omega_{RF})t} + J_8(m_a) e^{j(\omega_c + 8\omega_{RF})t}] \right\}^*, \quad (12)$$

where μ_{ph} is the responsivity of the photodiode. The above equation can be further simplified as follows:

$$I_{ph}(t) = \frac{\mu_{ph} \beta^2 |E_{MZM-D}(t)|^2}{4} \text{Cos}(16 \omega_{RF}t). \quad (13)$$

Thus, it can be seen mathematically through **Eq. 13** that the photo-detected output consists of an electrical signal of frequency 160 GHz as shown in the **Figure 4** which is 16 times the RF signal frequency, that is, 10 GHz being utilized at the CS.

RESULTS AND DISCUSSION

A polarization-controlled CWL emitting a light signal of frequency 193.1 THz is sent to MZM-A biased at MXTP and triggered through a 10 GHz RF signal. As MZM-A is biased at MXTP, its output contains only even order sidebands. The output from the first modulator is sent to the second, then to the third,

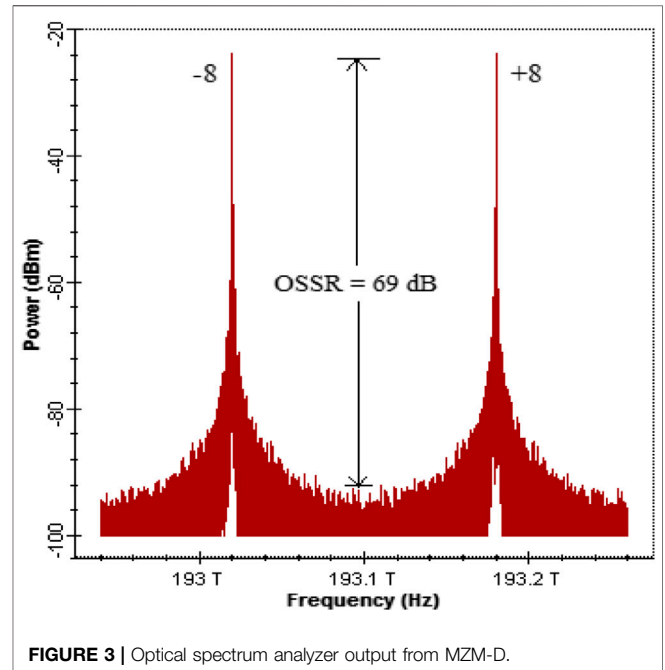
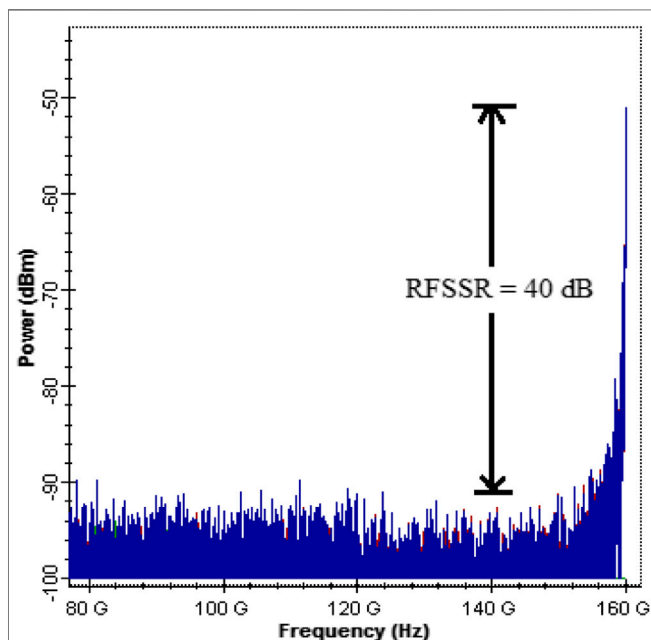


TABLE 2 | Simulation parameters employed for the present scheme of frequency 16 MM wave signal generation.

System block	Simulation parameters	Parameters value
Fiber link	Length	60 km
	Attenuation	0.22 dB/km
	Dispersion	16.75 ps/nm-km
	Dispersion slope	0.075 ps/nm ² /k
CW laser Diode	Frequency	193.1 THz
	Power	8 dBm
Local oscillator	RF signal	10 GHz
MZM modulator	MZM-A, B, and C extinction ratio	60 dB
	MZM-D extinction ratio	55 dB
	Insertion loss	3 dB
	Switching bias voltage	3.2
	Switching RF voltage	3.2
EDFA 1	Gain	10 dB
	Noise figure (NF)	3 dB
Amplifier	Gain	12 dB
	Noise figure	2 dB
PIN photodiode	PIN photodiode responsivity	0.9
	PIN dark current	9 nA

and at last to the fourth modulator in such a manner that the electrical phase shift of the RF local oscillator (LO) signal between first two consecutive MZMs is 45° and next two MZMs is 90° , and all the four modulators are biased at MXTP. By arranging the electrical phase shift, the modulation index, and the MZM in this manner, the output from the last modulator suppresses the carrier with all other spurious harmonics and contains only eighth-order SBs at $\omega_c + 8\omega_{RF}$, that is, 193.18 THz, and $\omega_c - 8\omega_{RF}$, that is, 193.02 THz with -22.4 dBm power. It can be

**FIGURE 4** | RF spectrum of the photo-detected signal from the PIN photodiode.

seen that the difference between +eighth (193.18 THz)- and -eighth (193.02 THz)-order SBs is the 16th multiple of the input electrical signal. These sidebands are then sent to the BS through a 60-km standard single-mode fiber (SSMF) with parameters mentioned in **Table 2**. At the BS, a hybrid configuration of cascaded amplifiers consisting of EDFA with gain of 10 dB and optical amplifier having 15 dB gain is utilized to mitigate the losses incurred during transmission over the fiber, and then a PIN photodiode with a responsivity of 0.9 A/W is utilized to detect the modulated signal by converting it back to electrical form and hence a 160-GHz signal is detected using the RF spectrum analyzer with tan output power of -50 dBm.

Impact of Nonideal Parameters on the OSSR and the RSSR

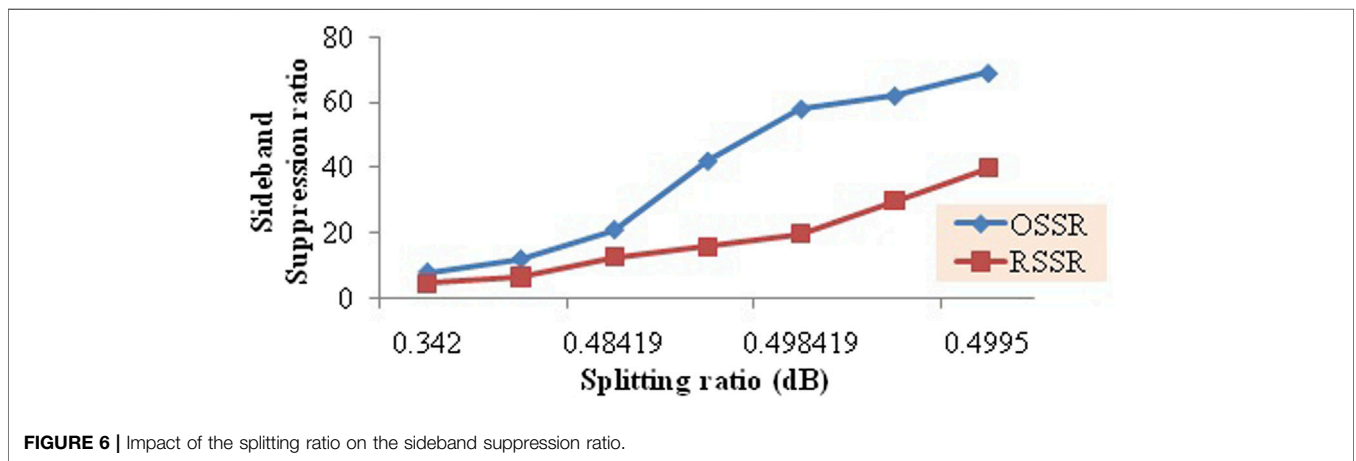
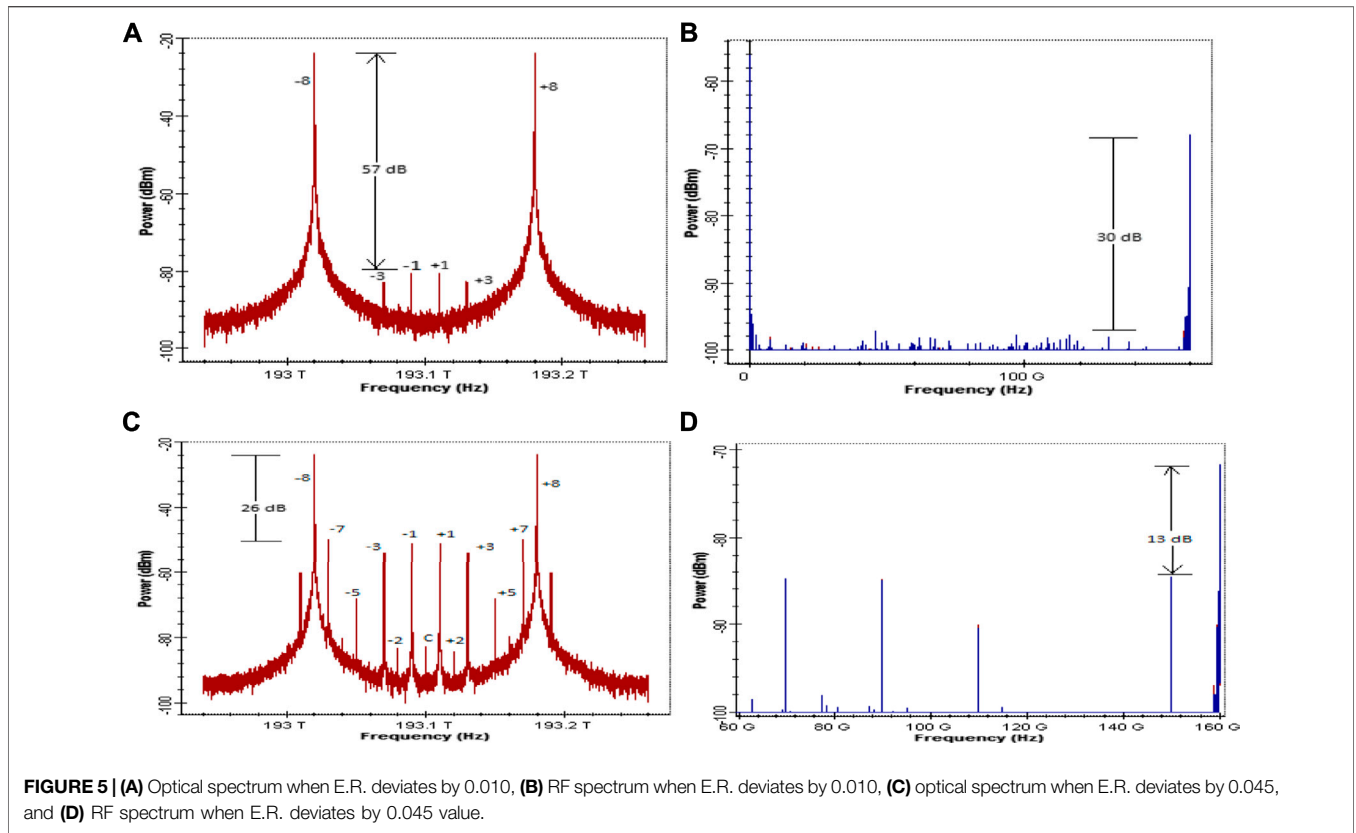
The above-mentioned results are based on the simulation carried over the OptiSystem software by assuming ideal parameters as mentioned in **Table 2**. However, these parameters might deviate from their desired values and thus it is crucial to analyze the impact of several nonideal parameters, such as RF voltage variation, the MZM extinction ratio, a cascaded amplifier configuration, and phase drift is analyzed over the OSSR and the RSSR.

Extinction Ratio and Splitting Ratio

For evaluating the proposed system performance, the impact of the extinction ratio (E. R.) or the splitting ratio of each MZM is studied over the OSSR and the RSSR, as shown in **Figure 5**. It is observed that as the extinction ratio varies from its ideal value, the system is not able to suppress the odd order SBs as P_8/P_1 is 57 dB when it deviates by 0.010 from the ideal value with 30 dB RSSR, and the eighth-order SBs are 26 dB greater than seventh order SBs when it deviates by a value of 0.045 with the 16-tupled MM wave being only 13 dB higher than the 15-tupled signal deteriorating the system performance, as shown in **Figure 5**. This states that the OSSR and the RSSR rises with an increasing splitting ratio/extinction ratio, as the splitting ratio is dependent on the extinction ratio of the MZM. Both the sideband suppression ratio (SSR) are maximum at 0.4995 splitting ratio, as calculated from **Eq. 3** under *Odd Order Harmonics Elimination*, and the unwanted sidebands are completely eliminated when the MZM extinction ratio is set to 60 dB being independent of the extinction ratio exceeding 60 dB, as clearly depicted in **Figures 6, 7**.

Modulation Index

The optical and RF spectrum when M.I. deviates 0.0588 from the ideal value is depicted in **Figure 8** where the P_8 is 14 dB higher than P_0 and 62 dB from P_3 , respectively. However, the 16-tupled MM wave is 11 dB greater than the octupling wave (eighth multiple of RF), which is quite less for the applications requiring MM wave for their operation. Besides this, the impact of the modulation index on the sideband power ratio (SBPR) (P_8/P_0) is depicted in **Figure 9**, which shows that the system provides (P_8/P_0) greater than 5 dB



and the RSSR greater than 2 dB (Figure 10) in the M.I. range of 2.678–2.945 by providing the peak of the OSSR [i.e., (P_8/P_0)] and the RSSR at an M.I. of 2.8258 with an RF voltage of 2.87989. The system provides an acceptable and tunable SSR which is greater than 15 dB in the M.I. ranging from 2.778 to 2.873.

Phase Drift Analysis of the OSSR

The effect of phase drift can be analyzed over the system by studying the OSSR deviation over the phase drift in PS. It can be noticed that for $\pm 10^\circ$ phase drift between MZM upper arm

and lower arms OSSR is above 25 dB which means that the system is less sensitive as far as MZM arms' phase drift is considered, while it is sensitive toward the phase drift in the phase shifters of the RF signal which drives the DD-MZM modulator, as depicted in Figure 11. However, the system provides acceptable performance for $\pm 8^\circ$ phase drift.

Cascaded Hybrid Amplifier Configuration

Amplifiers are used in the system so as to compensate the losses which are inserted while the signal travels through the optical

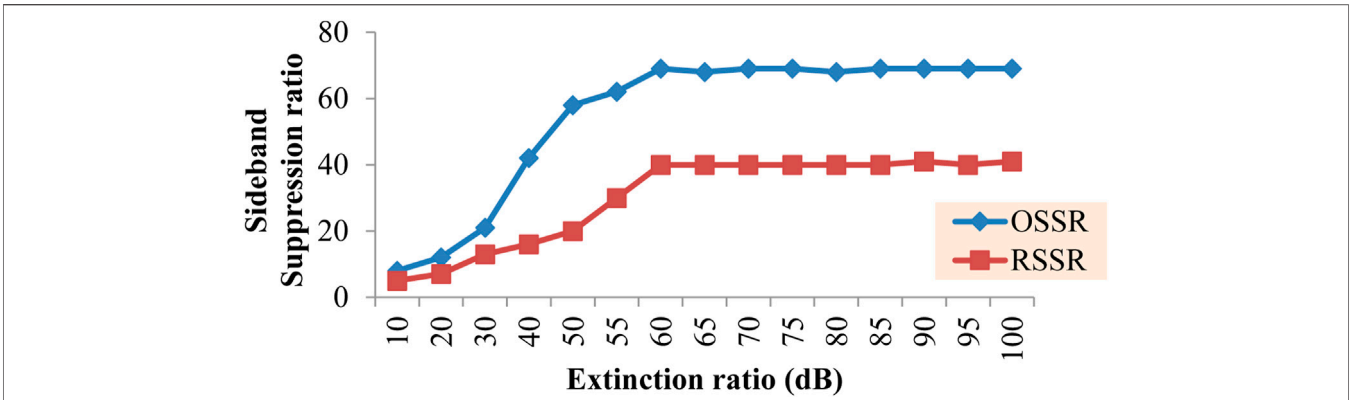


FIGURE 7 | Impact of the MZM extinction ratio on the sideband suppression ratio.

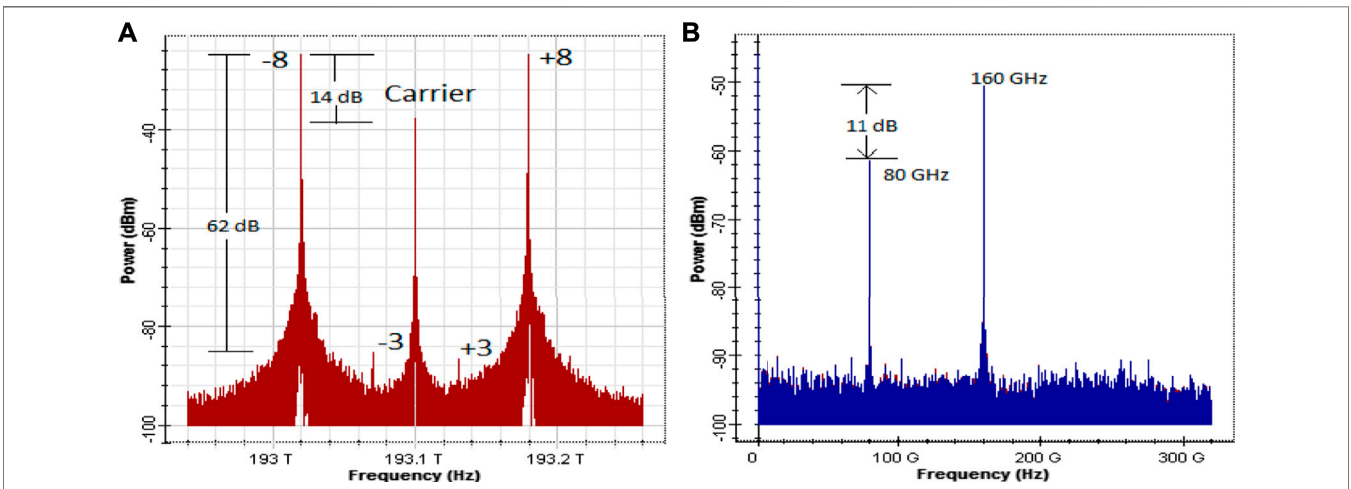


FIGURE 8 | (A) Optical spectrum and (B) RF spectrum output at M. I of 2.776.

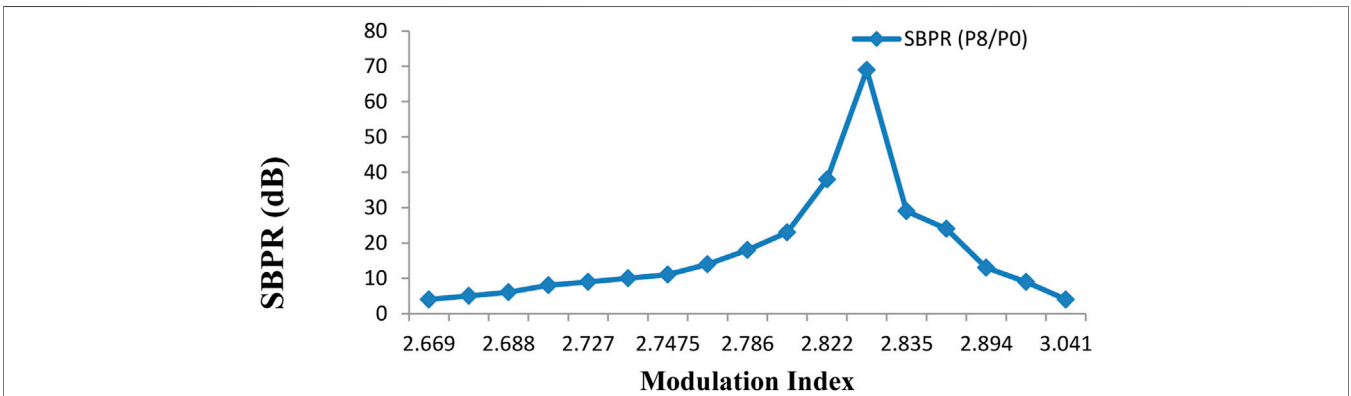
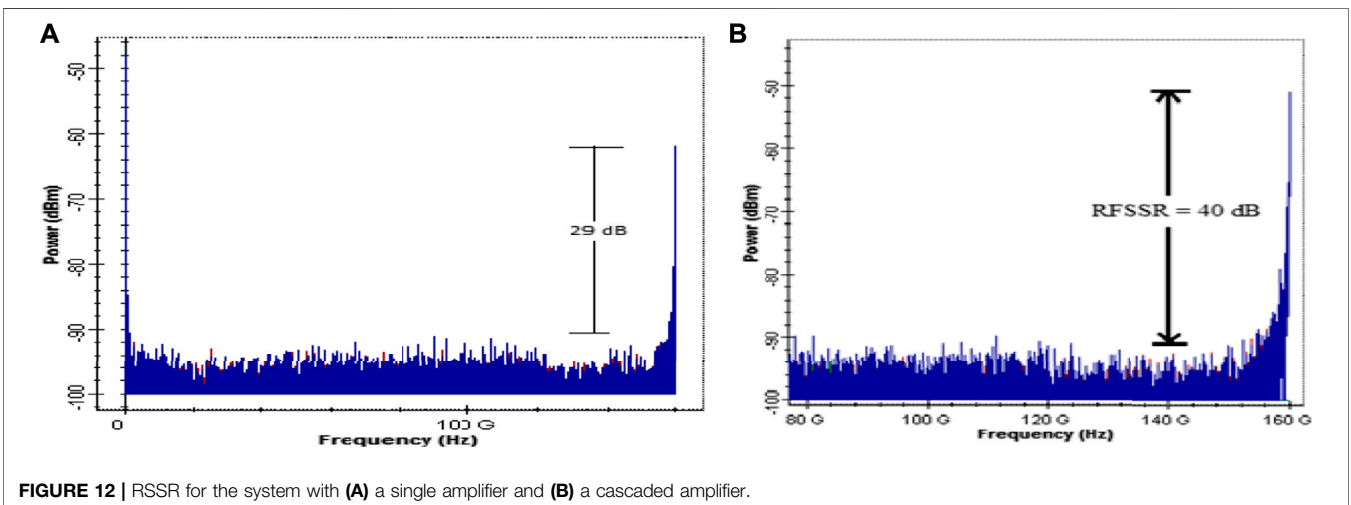
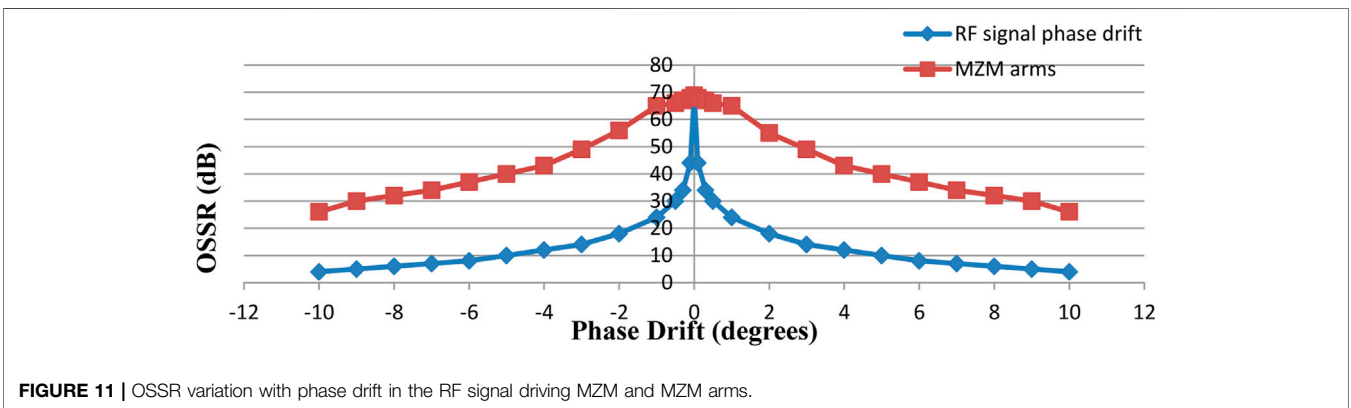
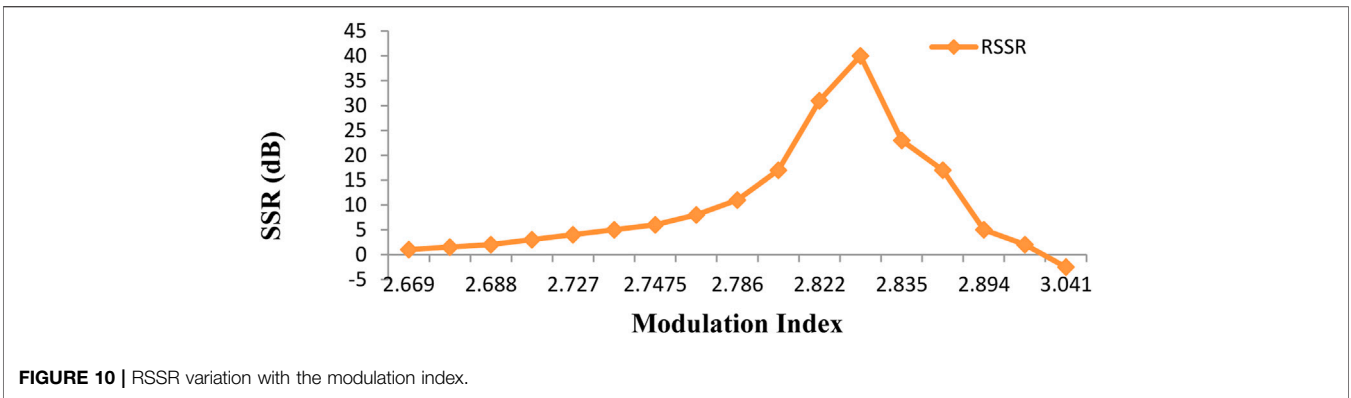


FIGURE 9 | SBPR variation with the modulation index.



fiber. The impact of using a cascaded amplifier configuration having EDFA 1 connected with optical amplifier with their parameters mentioned in **Table 2** enhances the RFSSR by 11 dB in comparison to a single amplifier configuration with a

20-dB gain and NF of 4 dB when detected by the PIN photodiode generates a 160-GHz with a 29-dB RFSSR, as shown in **Figure 12**. It can be noted that the cascaded amplifier configuration results in the improved RFSSR.

CONCLUSION

A photonic generation scheme of a frequency 16-tupled MM wave signal is presented and demonstrated using a series-connected DD-MZM with a double sideband optical carrier suppression modulation offering efficient power transmission. With appropriate adjustment of internal parameters, such as the modulation index, DC biasing, the splitting ratio, and electrical phase difference, and utilizing a hybrid amplifier configuration, a 160-GHz MM wave signal is generated from a 10-GHz RF signal with an OSSR of 69 dB and an RSSR of 40 dB. This system does not require any additional circuitry such as a mixer, a filter, and a digital signal processor. In comparison to the previous approaches, the proposed structure optically generates a highly conversant, spectrally pure 16-tupled MM wave signal with a better tunable OSSR and an RSSR and with a wider tunable range from 1–15 GHz, as there is no filter required in this scheme. Further, the system provides

acceptable performance with a wider range of M.I. variation 2.778–2.873, $\pm 8^\circ$ phase drift between MZM arms, and electrical phase shifters and is independent of the extinction ratio beyond 60 dB.

DATA AVAILABILITY STATEMENT

The original contributions presented in the study are included in the article/Supplementary Material; further inquiries can be directed to the corresponding author.

AUTHOR CONTRIBUTIONS

SD proposed the idea and supervised the whole work. Asha carried out the modeling and simulation. Both authors contributed to the writing of the manuscript.

REFERENCES

- Zeb K. *Photonic generation of spectrally pure Millimeter wave signals for 5G applications*. Ottawa, Canada: IEEE International Topical Meeting on Microwave Photonics (2020). p. 1–4.
- Perez Galacho D, Sartiano D, and Sales S. Analog radio over fiber links for future 5G radio access networks. *IEEE ICTON* (2019) 1–4. doi:10.1109/icton.2019.8840516
- He X. Linear analog photonic link enabled RoF-5G front haul transmission system. *Optik* (2019) 183(3):99–104. doi:10.1016/j.ijleo.2019.02.056
- Kamissoko D, Jing H, Ganame H, and Tall M. Performance investigation of W-band Millimeter wave radio over fiber system employing optical heterodyne generation and self homodyne detection. *Opt Commun* (2020) 474(1):1–8. doi:10.1016/j.optcom.2020.126174
- Asha SD. A Comprehensive Review of Millimeter wave based radio over fiber for 5G front haul transmissions. *Ijst* (2021) 14(1):86–100. doi:10.17485/ijst/v14i1.2177
- Zhu Z, Zhao S, Chu X, and Dong Y. Optical generation of millimeter-wave signals via frequency 16-tupling without an optical filter. *Opt Commun* (2015) 354(1):40–7. doi:10.1016/j.optcom.2015.05.035
- Li X, Zhao S, Zhu Z, Gong B, Chu X, Li Y, et al. An optical millimeter-wave generation scheme based on two parallel dual-parallel Mach-Zehnder modulators and polarization multiplexing. *J Mod Opt* (2015) 62(18):1502–9. doi:10.1080/09500340.2015.1045948
- Ying X, Xu T, Li W, Weng H, and Zhang X. Photonic generation of millimeter-wave signal via frequency 16-tupling based on cascaded dual – parallel MZM. *J Optoelectronics – Laser* (2017) 28(11):1212–7.
- Dar AB, Ahmad F, and Jha RK. Filterless 16-Tupled Optical Millimeter-wave Generation Using Cascaded Parallel Mach-zehnder Modulators with Extinction Ratio Tolerance. *PIER Lett* (2020) 91(1):129–35. doi:10.2528/pierl20031009
- Muthu K, Raja A, and Shanmugapriya G. Frequency 16-tupled optical millimeter wave generation using dual cascaded MZMs and 2.5 Gbps RoF transmission. *Optik* (2017) 14(1):338–46.
- Esakki Muthu K, and Sivanantha Raja A. Bidirectional MM-Wave Radio over Fiber transmission through frequency dual 16-tupling of RF local oscillator. *J Eur Opt Soc – Rapid Publications*. (2016) 12(24):1–9. doi:10.1186/s41476-016-0028-2
- Chen H, Ning T, Jian W, Pei L, and Li J. D-band millimeter-wave generator based on a frequency 16-tupling feed-forward modulation technique. *Opt Eng* (2013) 52(1):0761041–4. doi:10.1117/1.oe.52.7.076104
- Wang D, Tang X, Xi L, Zhang X, and Fan Y. A filterless scheme of generating frequency 16-tupling millimeter-wave based on only two MZMs. *Opt Laser Tech* (2019) 116(1):7–12. doi:10.1016/j.optlastec.2019.03.009
- Baskaran M, and Prabakaran R. Optical Millimeter wave signal generation with frequency 16 tupling using cascaded MZMs and no optical filtering for radio over fiber system. *J Eur Opt Society-Rapid Publications* (2018) 14(13):1–8. doi:10.1186/s41476-018-0080-1

Conflict of Interest: The authors declare that the research was conducted in the absence of any commercial or financial relationships that could be construed as a potential conflict of interest.

Publisher's Note: All claims expressed in this article are solely those of the authors and do not necessarily represent those of their affiliated organizations, or those of the publisher, the editors and the reviewers. Any product that may be evaluated in this article, or claim that may be made by its manufacturer, is not guaranteed or endorsed by the publisher.

Copyright © 2021 Asha and Dahiya. This is an open-access article distributed under the terms of the Creative Commons Attribution License (CC BY). The use, distribution or reproduction in other forums is permitted, provided the original author(s) and the copyright owner(s) are credited and that the original publication in this journal is cited, in accordance with accepted academic practice. No use, distribution or reproduction is permitted which does not comply with these terms.